This article has been accepted for inclusion in a future issue of this journal. Content is final as presented, with the exception of pagination.

Cooperative Eco-Driving at Signalized Intersections in a Partially Connected and Automated Vehicle Environment

Ziran Wang, *Student Member, IEEE*, Guoyuan Wu, *Senior Member, IEEE*, and Matthew J. Barth, *Fellow, IEEE*

***Abstract*— The emergence of connected and automated vehicle (CAV) technology has the potential to bring a number of benefits to our existing transportation systems. Specifically, when CAVs travel along an arterial corridor with signalized intersections, they can not only be driven automatically using pre-designed control models but can also communicate with other CAVs and the roadside infrastructure. In this paper, we describe a cooperative eco-driving (CED) system targeted for signalized corridors, focusing on how the penetration rate of CAVs affects the energy efficiency of the traffic network. In particular, we propose a role transition protocol for CAVs to switch between a leader and following vehicles in a string. Longitudinal control models are developed for conventional vehicles in the network and for different CAVs based on their roles and distances to intersections. A microscopic traffic simulation evaluation has been conducted using PTV VISSIM with realistic traffic data collected for the City of Riverside, CA, USA. The effects on traffic mobility are evaluated, and the environmental benefits are analyzed by the U.S. Environmental Protection Agency's MOtor Vehicle Emission Simulator (MOVES) model. The simulation results indicate that the energy consumption and pollutant emissions of the proposed system decrease, as the penetration rate of CAVs increases. Specifically, more than 7% reduction on energy consumption and up to 59% reduction on pollutant emission can be achieved when all vehicles in the proposed system are CAVs.**

***Index Terms*— Connected and automated vehicles (CAVs), eco-driving, eco-approach and departure (EAD), cooperative adaptive cruise control (CACC), signalized intersections, mixed traffic.**

I. Introduction and Background

MOBILITY, safety and sustainability are all critical measures of performance in the field of transportation. In recent years, increased transportation activity continues to have significant impacts on the above measures and raises awareness and concerns from the general public. In terms of traffic mobility, drivers in the U.S. spent an average of 41 hours a year in traffic during peak hours in 2017, costing nearly $305 billion in total, which equals to $1,445 per driver [1]. In terms of traffic safety, it is estimated that 37,461 people died in accidents in the U.S. involving motor vehicles in 2016, which endured a 6 percent rise from the year before [2]. And in terms of environmental sustainability, the transportation sector was the second largest producer of GHG nationwide, accounting for approximately 27% of total U.S. emissions in 2013 [3].

In recent years, there has been a significant amount of research interest on how to improve the mobility, safety and sustainability of signalized intersections. Specifically, connected and automated vehicle (CAV) technology has been widely studied to improve the sustainability of transportation systems, where a CAV can be driven by itself with the help of its on-board perception sensors, and also communicate with the driver, other vehicles on the road (through vehicle-to-vehicle, i.e., V2V communications), roadside infrastructure (through vehicle-to-infrastructure, i.e., V2I communications), and the "Cloud" [4]. Such applications are often categorized as eco-driving at signalized intersections, with specific names such as GLOSA (Green Light Optimized Speed Advisory (GLOSA) or Eco-Approach and Departure (EAD) [5]–[10]. On top of the advanced technology on the vehicle side, some researchers also focus on the infrastructure side to improve the overall energy efficiency of the traffic system. Lee *et al.* proposed a cooperative vehicle intersection control system that enables cooperation between vehicles and infrastructure for effective intersection operations and management [11]. Guler *et al.* developed a CAV-based algorithm considering platooning and signal flexibility to gain traffic mobility benefits [12]. A real-time adaptive signal phase allocation algorithm was proposed by Feng *et al.* using CAV data, and the results showed a reduction of 16.33% in terms of total delay [13].

In addition to sustainability benefits, CAV technology can also produce significant mobility and safety benefits. One major application of the CAV technology is the cooperative adaptive cruise control (CACC) system, which enables CAVs to cooperate with each other to form vehicle strings. Numerous works on the mobility and safety perspectives of CACC systems have been conducted [14]–[21]. Researchers have also integrated eco-driving technology with CACC systems for traffic at signalized intersections. An Eco-CACC algorithm for isolated signalized intersection was developed by Yang *et al.*, which computes the fuel-optimum vehicle trajectory to ensure that a CAV arrive at the intersection as soon as the last CAV in the queue is discharged [22]. Xie *et al.* developed a model of heterogeneous traffic with a mix of regular and connected vehicles [23]. CACC and intelligent traffic signal

Manuscript received September 16, 2018; revised January 2, 2019 and March 22, 2019; accepted April 14, 2019. The Associate Editor for this paper was M. Menendez. *(Corresponding author: Ziran Wang.)*

The authors are with the Bourns College of Engineering-Center for Environmental Research and Technology (CE-CERT), University of California at Riverside, Riverside, CA 92507 USA (e-mail: zwang050@ucr.edu).

Digital Object Identifier 10.1109/TITS.2019.2911607

1524-9050 © 2019 IEEE. Personal use is permitted, but republication/redistribution requires IEEE permission.
See http://www.ieee.org/publications_standards/publications/rights/index.html for more information.

Authorized licensed use limited to: Univ of Calif Riverside. Downloaded on April 14,2020 at 21:38:26 UTC from IEEE Xplore. Restrictions apply.

This article has been accepted for inclusion in a future issue of this journal. Content is final as presented, with the exception of pagination.

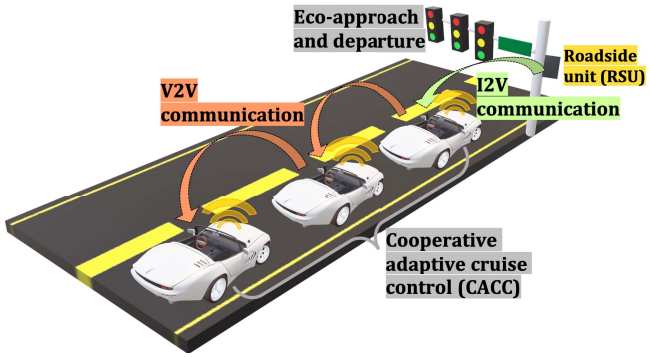

Fig. 1. Illustration of the proposed cooperative eco-driving system.

control technology were integrated by Malakorn *et al.*, where the mobility, energy and environmental impacts of the proposed system were analyzed [24]. A cluster-wise cooperative EAD application at isolated intersections was developed by our previous work, where CAVs are formed into different clusters based upon CACC protocols, and conduct eco-driving towards the intersection in a collaborative manner [25]. In this work, we further improve the system by considering partially CAV environment instead of a pure CAV environment, and develop the system for signalized intersections along a corridor instead of a single intersection. We further test our proposed system in microscopic traffic simulations instead of numerical simulations.

The remainder of this paper is organized as follows: Section II illustrates the overall framework, specifications and assumptions of our proposed system. Section III proposes a role transition protocol for cooperative eco-driving (CED) vehicles in the system. Section IV demonstrates different longitudinal control models developed for different vehicle types in the system. A simulation study of the proposed system has been conducted using microscopic traffic simulator PTV VISSIM, and its results are evaluated and analyzed in Section V [26]. Section VI concludes this paper together with further discussion on future work.

II. Problem Statement

The objective of this study is to develop a CED system by CAV technology to improve the energy efficiency along a corridor with signalized intersections. To study the effect of penetration rate of CAVs, we define two different types of vehicles in the system as conventional vehicles and CED vehicles. Different role transition protocols and longitudinal control models are proposed for different vehicles based on their degrees of connectivity and automation. In this study, a microscopic traffic simulation network is modeled in VISSIM, where different vehicle longitudinal control models and their relevant logic (e.g., role transition) are integrated into simulation network to simulate vehicles' behavior, and an energy/emission model is implemented to analyze the environmental impacts of proposed methodologies.

The proposed cooperative eco-driving system can be illustrated as Fig. 1. Note that our study mainly focuses on designing an integrated traffic system with proposed control protocol, so some reasonable specifications and assumptions

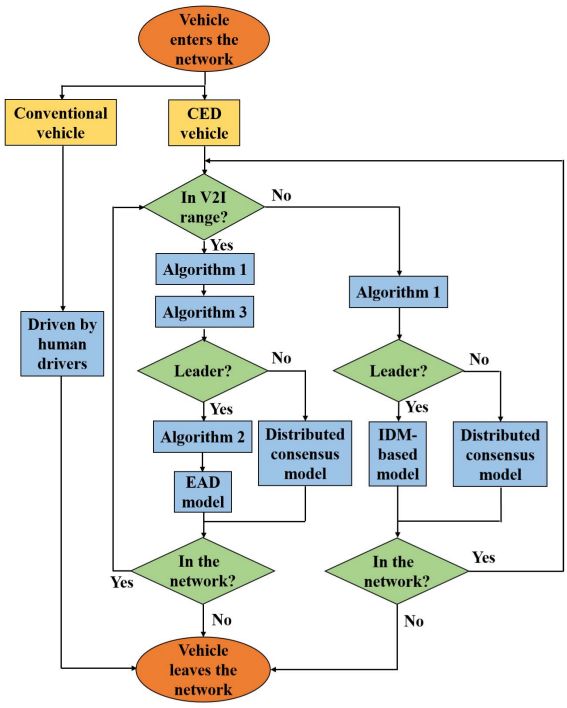

Fig. 2. General framework of the proposed eco-driving system.

are made as follows to quantify the potential benefits while modeling the system:

1) All CED vehicles in the proposed system are equipped with appropriate on-board sensors (e.g., OBD, camera, radar, LIDAR, etc.), and their measurements and calculations are precise without error.
2) All CED vehicles are V2V-enabled, which are equipped with wireless communication devices such as Dedicated Short Range Communications (DSRC) on-board units (OBUs), to transmit vehicle information among each other, and also V2I-enabled, which can receive MAP and SPaT (Signal Phase and Timing) information from intersections.
3) All intersections in the system are equipped with DSRC roadside units (RSU) to broadcast their MAP and SPaT message, and all signals are fixed-timing control.
4) We focus on the development of longitudinal control strategies and application in the simulation study. The lateral maneuvers rely on the default lane change model of VISSIM.

The general framework of the proposed system can be seen in Fig. 2. All models and algorithms are introduced in section III and IV of this paper.

Compared to similar existing studies in this research area, such as [27]–[29], our system has the following improvements:

1) Most current works assume 100% penetration rate of CAVs in the systems, which are unrealistic for real-world implementations. Further, we not only consider two different types of vehicles, but also model the interactions between different vehicle types. For example, we study how a CED vehicle will response when a conventional vehicle suddenly moves in front of it.
2) Different from most literatures that consider CAVs as different individual system that conducts eco-driving

Authorized licensed use limited to: Univ of Calif Riverside. Downloaded on April 14,2020 at 21:38:26 UTC from IEEE Xplore. Restrictions apply.

This article has been accepted for inclusion in a future issue of this journal. Content is final as presented, with the exception of pagination.

maneuver by itself, our work proposes a cooperative eco-driving system, where different CAVs are categorized by different roles. Generally, leaders conduct eco-driving maneuver with respect to signals through V2I communication, while followers follow leaders' maneuvers through V2V communications. Therefore, less conflicts will be generated among different CAVs due to their collaborations.

3) Instead of studying the eco-approaching maneuver on only one direction of one isolated signalized intersection, we model a corridor with two signalized intersections and all four directions, so both eco-approach and eco-departure maneuvers are developed and analyzed. The proposed algorithms allow CED vehicles to reset their parameters once passing the current intersection, and update parameters again while entering the V2I communication range of the next intersection.
4) Rather than just numerical simulations, we conduct microscopic traffic simulation based on the University Avenue corridor in Riverside, CA, with real-world traffic flow and signal timing data provided by the government. Therefore, the results of implementing the proposed CAV technology on the current transportation system would be more realistic and convincing.

III. Vehicle Role Transition Protocol

In the proposed system, there are generally two types of passenger vehicles: conventional vehicles and CED vehicles. Conventional vehicles are assumed to be driven by human drivers with no degree of connection and automation. CED vehicles are assumed to be CAVs with appropriate on-board sensors to conduct automated driving, and OBUs to transmit information among vehicles and receive information from the infrastructure. A vehicle role transition protocol is proposed for V2X-enabled vehicles as *Algorithm 1*, since a CED vehicle can transit from a leader to a follower in a vehicle string, or vice versa.

A CED vehicle continuously checks whether there is a preceding vehicle on the same lane, and within the V2V communication range. If no, then it is a leader of a string. If yes, then it compares the distance to the preceding CED vehicle with the distance to the intersection. If the preceding vehicle already passes the intersection, then the ego-vehicle is a CED leader. If not, then it further checks the time-to-collision value (if the preceding vehicle is a conventional vehicle), or checks the estimated time-to-arrival at the intersection (if the preceding vehicle is also a CED vehicle).

If the preceding vehicle is a conventional vehicle and the time-to-collision value is lower than a certain threshold, it means the CED vehicle has a high chance to get a front-bumper-to-rear-bumper collision with its preceding conventional vehicle, so the CED vehicle will be a follower to follow its preceding conventional vehicle's movement.

If the preceding vehicle is also a CED vehicle and the difference between two consecutive CED vehicles' time-to-arrival is larger than a certain threshold (normally the total length of an amber phase and a red phase), then the following CED vehicle may be considered as the "string breaker" scenario and becomes a CED leader. The method to calculate estimated time-to-arrival can be found in *Algorithm 2*and *Algorithm 3*.

Algorithm 1: Role Transition of CED Vehicles

```
Input: inter-vehicle distance d_gap, distance to
       the intersection d_1, time-to-arrival of
       the ego vehicle t^arr, time-to-arrival of
       the preceding vehicle t^arr_pre,
       time-to-collision with respect to the
       preceding vehicle t^collision
Output: vehicle role
for all CED vehicles do
  if d_gap < V2V range then
    if d_gap > d_1 then
      ego vehicle is a CED leader
    else
      if preceding is a CED vehicle then
        if (t^arr − t^arr_pre) ≥ threshold then
          ego vehicle is a CED leader
        else
          ego vehicle is a CED follower
        end if
        if (t^collision) < threshold then
          ego vehicle is a CED follower
        else
          ego vehicle is a CED leader
        end if
      else
        end if
    end if
  else
  end if
  ego vehicle is a CED leader
end for
```

Essentially, the "string breaker" scenario happens when two consecutive CED vehicles' time-to-arrival fall into two different green windows. Since we take green windows into account when calculating the time-to-arrival values, it is possible that the preceding one of two neighboring CED vehicles estimates to reach the intersection at the end of the preceding green window, but the following vehicle estimates to arrive at the start of the following green window. Therefore, a "string breaker" scenario is created, where the following CED vehicle becomes a CED leader, and conducts its own EAD movement through the intersection.

IV. Longitudinal Control Model

A. Conventional Vehicle Longitudinal Control Model

In the proposed system, conventional vehicles are assumed to be driven by human drivers, which are not equipped with any on-board sensor or OBU. Therefore, the car-following model originally proposed by Rainer Wiedemann in 1974 (i.e., Wiedemann 74) is used to model the longitudinal behaviors of conventional vehicles [30].

The safety clearance is defined in Wiedemann 74 as

$$d = a \cdot x = (b \cdot x_{add} + b \cdot x_{mult} \cdot z) \cdot \sqrt{v} \tag{1}$$

where $a \cdot x$ denotes the average standstill distance; $b \cdot x_{add}$ is the additive part of safety distance; $b \cdot x_{mult}$ is the multiplicative part of safety distance; v is the speed of vehicle; z is a value of range [0, 1]. The tolerance of $a \cdot x$ lies between ± 0.1 m which is normally distributed at around 0 m, with a standard

Authorized licensed use limited to: Univ of Calif Riverside. Downloaded on April 14,2020 at 21:38:26 UTC from IEEE Xplore. Restrictions apply.

This article has been accepted for inclusion in a future issue of this journal. Content is final as presented, with the exception of pagination.

deviation of 0.3 m. Both $b \cdot x_{add}$ and $b \cdot x_{mult}$ allow to adjust the time requirement values.

B. CED Vehicle Longitudinal Control Model

For modeling purposes, a CED vehicle can be separated into two different components: the CED vehicle longitudinal control model that delivers reference values of vehicle acceleration, and a vehicle powertrain model that transforms reference acceleration values into realized throttle or brake values. In this part, we mainly focus on the longitudinal control model, which generates the acceleration reference demand and then feeds it into the powertrain model.

1) CED Leader When Out of the V2I Range: When the CED leader is running out of the V2I communication range of the intersection, it follows its desired speed while there is no preceding conventional vehicle in a certain range, or follows the preceding conventional vehicle while there is one. In the proposed system, the Intelligent Driver Model (IDM)-based longitudinal control strategy is applied to the longitudinal movement of the CED leader when out of V2I range of intersections.

IDM was proposed by Treiber *et al.* [31] and has been widely studied in many research work. In this study, we develop a longitudinal control model for the CED leader (in the case of outside the V2I communication range) based upon IDM, which can be given as

$$a_{ref} = a_{max} \cdot \left[1 - \left(\frac{v_{ego}}{v_{des}} \right)^{\delta} - \Sigma \right] \tag{2}$$

where $\Sigma = \left(\frac{d_{safe} + v_{ego} \cdot t_{gap} + \frac{v_{ego} \cdot (v_{ego} - v_{pre})}{2 \cdot \sqrt{a_{max}^2}}}{d_{gap}}\right)^2$ is the correlation term with the front vehicle, which has a value when there is a conventional vehicle gets in front of the CED leader, and equals to 0 when no other vehicle is in front. a_{max} is a preset constant which denotes the maximum changing rate of speed; v_{ego} denotes the current speed of the ego vehicle; v_{pre} denotes the current speed of its preceding vehicle; v_{des} is a preset constant which denotes the desired speed of the ego vehicles; d_{safe} is a preset constant which denotes the minimum allowed inter-vehicle distance; t_{gap} is a preset constant which denotes the desired time gap; d_{gap} denotes the measured inter-vehicle distance between the ego vehicle and its preceding vehicle. The free acceleration exponent δ is defined based upon IDM, which characterizes how the acceleration of the ego vehicle decreases with speed (e.g., $\delta = 1$ corresponds to a linear decrease, and $\delta \to \infty$ leads to a constant acceleration).

2) CED Leader When in the V2I Range: Different from the case when running out of the V2I communication range of the intersection, the CED leader can receive MAP and SPaT information from upcoming intersections while it is in the V2I range, and is able to conduct EAD movement through intersections accordingly. In the proposed system, we develop a piecewise trigonometric-linear EAD algorithm based upon our previous work to control the longitudinal movements of the CED leader when in the V2I range. Similar to previous segments, we mainly focus on the longitudinal control model that generates the acceleration reference demand and then feeds it into the dynamics model.

We define four different EAD scenarios for a CED leader when it is in the V2I communication range of the intersection, which are accelerate scenario, cruise scenario, decelerate scenario, and stop scenario. Once the CED leader receives the SPaT information from the intersection and combines that with the MAP information, it calculates the following variables to decide which scenario it should be in:

$$t_c = \frac{d_1}{v_1} \tag{3}$$

$$t_e = \frac{d_1 - v_1 \cdot \frac{\pi}{2\alpha}}{v_{lim}} + \frac{\pi}{2\alpha} \tag{4}$$

$$t_l = \frac{d_1 - v_1 \cdot \frac{\pi}{2\beta}}{v_{coast}} + \frac{\pi}{2\beta} \tag{5}$$

$$\alpha = \min\left\{ \frac{2 \cdot a_{max}}{v_{lim} - v_1}, \sqrt{\frac{2 \cdot jerk_{max}}{v_{lim} - v_1}} \right\} \tag{6}$$

$$\beta = \min\left\{ \frac{2 \cdot a_{max}}{v_1 - v_{coast}}, \sqrt{\frac{2 \cdot jerk_{max}}{v_1 - v_{coast}}} \right\} \tag{7}$$

where t_c, t_e and t_l stand for cruising time-to-arrival, earliest time-to-arrival, and latest time-to-arrival, respectively; α and β are variables to calculate t_e and t_l, respectively; d_1 denotes the current distance to the intersection; v_1 denotes the current speed of vehicle; $jerk_{max}$ is a preset constant which denotes the maximum changing rate of acceleration or deceleration; v_{lim} is a preset constant which denotes the speed limit of the current roadway; v_{coast} is a preset constant which denotes the coasting speed. If the current signal phase is green, then we can define the available green window as $T = [0, t_{curr\_e}) \bigcup [t_{next\_s}, t_{next\_e})$; If the current signal phase is red, then $T = [t_{next\_s}, t_{next\_e})$. Note t_{curr_e} denotes time-to-the-end-of-current-green-window, t_{next_s} and t_{next_e} denote time to-the-start-of-next-green-window and time-to-the-end-of-next-green-window, respectively. Then the EAD scenario identification protocol can be demonstrated as *Algorithm 2*.

Algorithm 2: EAD Scenario Identification of the CED Leader When in the V2I Range

Input: available green window T, cruising time-to-arrival t_c, earliest time-to-arrival t_e, latest time-to-arrival t_l
Output: EAD scenario, estimated time-to-arrival t_{arr}

for *all CED leaders in the V2I range* **do**
  if $t_c \in T$ **then**
    cruise scenario, $t_{arr} = t_c$
  else if $[t_e, t_c] \cap T \neq \emptyset$ **then**
    accelerate scenario, $t_{arr} = \min[t_e, t_c] \cap T$
  else if $[t_c, t_l] \cap T \neq \emptyset$ **then**
    decelerate scenario, $t_{arr} = \min[t_c, t_l] \cap T$
  else
    stop scenario, $t_{arr} = t_{next\_s}$
  end if
end for

Once the EAD scenario of the CED leader is identified by *Algorithm 2*, the CED leader will adopt different longitudinal control models with respect to different scenarios.

Authorized licensed use limited to: Univ of Calif Riverside. Downloaded on April 14,2020 at 21:38:26 UTC from IEEE Xplore. Restrictions apply.

This article has been accepted for inclusion in a future issue of this journal. Content is final as presented, with the exception of pagination.

If the CED leader is categorized into the cruise scenario, it means this vehicle can travel through the intersection during the green phase without any speed change. Therefore, the reference longitudinal acceleration of this vehicle is zero.

If the CED leader is categorized into the accelerate or decelerate scenario, the vehicle needs to firstly accelerate or decelerate to a certain speed while approaching the intersection. This takes a half period of the trigonometric algorithm, where the reference acceleration of the CED leader during the first quarter period $t \in \left[0,\ \frac{\pi}{2j_1}\right)$ is

$$a_{ref} = v_{d1} \cdot j_1 \cdot \sin\left(j_1 t\right) \tag{8}$$

followed by the second quarter period $t \in \left[\frac{\pi}{2j_1},\ \frac{\pi}{2j_1} + \frac{\pi}{2k_1}\right)$

$$a_{ref} = v_{d1} \cdot j_1 \cdot \sin\left[k_1 \cdot \left(t + \frac{\pi}{k_1} - t_1\right)\right] \tag{9}$$

Upon finishing the first half of the trigonometric algorithm, the CED leader maintains a constant speed and approaches the intersection. When the CED leader departs the intersection, it decelerates or accelerates to the target speed (if $v_h \neq v_{tar}$), which takes the other half period of this trigonometric algorithm. The reference acceleration during the third quarter period $t \in \left[t_{depart},\ t_{depart} + \frac{\pi}{2k_2}\right)$ is

$$a_{ref} = v_{d2} \cdot j_2 \cdot \sin\left[k_2 \cdot \left(t + \frac{\pi}{k_2} - t_{depart}\right)\right] \tag{10}$$

followed by the last quarter period $t \in \left[t_{depart} + \frac{\pi}{2k_2}, t_{depart} + \frac{\pi}{2j_2} + \frac{\pi}{2k_2}\right)$

$$a_{ref} = v_{d2} \cdot j_2 \cdot \sin\left[j_2 \cdot \left(t - t_{depart} - \frac{\pi}{2j_2} - \frac{\pi}{2k_2}\right)\right] \tag{11}$$

In above equations, $v_h = \frac{d_1}{t^{arr}}$, $v_{d1} = v_h - v_1$, $v_{d2} = v_h - v_{tar}$, where v_{tar} is a preset constant that denotes the target speed while departing the intersection; $t_{depart} = \frac{d_2}{v_h}$ denotes time-to-departure; d_2 is a preset constant that denotes the departure distance; k_i and j_i are gains to control the changing rate of acceleration or deceleration, which can be obtained by solving the following optimization problem.

$$\max_{i=1,2} \ k_i \tag{12a}$$

subject to

$$\begin{aligned} |k_i \cdot v_{di}| &\leq a_{max} \\ |{k_i}^2 \cdot v_{di}| &\leq jerk_{max} \\ k_i &\geq \left(\frac{\pi}{2} - 1\right) \cdot \frac{v_h}{d_i} \end{aligned} \tag{12b}$$

since the vehicle dynamics should subject to the hard constraint of vehicle powertrain's ability, and ride comfort of human passengers. Once k_i is solved, j_i can be calculated by

$$j_i = \frac{-\frac{\pi}{2}k_i - \sqrt{\left(\frac{\pi}{2}k_i\right)^2 - 4{k_i}^2 \cdot \left[\left(\frac{\pi}{2} - 1\right) - \frac{d_i}{v_h} \cdot k_i\right]}}{2\left[\left(\frac{\pi}{2} - 1\right) - \frac{d_i}{v_h} \cdot k_i\right]}, \quad (i = 1, 2) \tag{13}$$

If the CED leader is categorized into the stop scenario, it means the vehicle cannot avoid the red phase by either accelerating or decelerating. The vehicle needs to firstly decelerate all the way to full stop while approaching the intersection, and then accelerate to the target speed while departing. The reference acceleration of the CED leader in this scenario is also calculated by equation (8) – (11), with

$$t_{depart} = t_{next\_s} \tag{14}$$

$$v_h = \frac{v_1}{2} \tag{15}$$

$$k_i = j_i = \frac{v_h}{d_i} \cdot \pi \tag{16}$$

It should be noted that while the CED leader is in the V2I range and is conducting the EAD maneuver, it also continuously runs *Algorithm 1* to check whether potential role transition is needed. There are chances that other vehicles cut in front of the CED leader, so the CED leader will transform into a CED follower and will no longer adopt the piecewise trigonometric-linear EAD algorithm to control its longitudinal movement. If the role of the CED leader stays unchanged, it will still apply EAD algorithm.

3) CED Follower: When the CED follower is out of the V2I communication range of the intersection, the distributed consensus algorithm is proposed to control its longitudinal movement, which is based upon the distance difference and the speed difference between the ego vehicle and the preceding vehicle. The reference acceleration of the ego vehicle is calculated by the second-order consensus algorithm as

$$a_{ref} = \beta \cdot (d_{gap} - d_{ref}) + \gamma \cdot (v_{pre} - v_{ego}) \tag{17}$$

where β and γ are damping gains; d_{ref} denotes the reference inter-vehicle distance, which can be calculated as

$$d_{ref} = min(d_{gap}, d_{safe}) \tag{18}$$

where d_{gap} denotes a time gap-based inter-vehicle distance, which is calculated by the product of ego vehicle's current speed and desired time gap, stated as

$$d_{gap} = v_{ego} \cdot t_{gap} \tag{19}$$

When ego vehicle's speed is very low (e.g., $v_{ego} \rightarrow 0$), the reference inter-vehicle distance returned by d_{time} is also very low, which might lead to front-to-rear collision. Therefore, a minimum allowed inter-vehicle distance d_{safe} is defined to ensure the reference inter-vehicle distance is always higher than a threshold value.

When the CED follower is in the V2I range, it needs to continuously calculate its estimated time-to-arrival based on Algorithm 3. While running Algorithm 3, the CED follower also runs Algorithm 1 with the updated estimated time-to-arrival calculated from Algorithm 3. Some certain outcomes of Algorithm 3 will trigger a role transition in Algorithm 1, which was mentioned earlier in section III as the "string breaker" scenario. In that case, the CED follower will transform into a CED leader and will no longer adopt the distributed consensus algorithm to control its longitudinal movement. If the role of the CED follower stays unchanged, it will still apply the distributed consensus algorithm.

Authorized licensed use limited to: Univ of Calif Riverside. Downloaded on April 14,2020 at 21:38:26 UTC from IEEE Xplore. Restrictions apply.

This article has been accepted for inclusion in a future issue of this journal. Content is final as presented, with the exception of pagination.

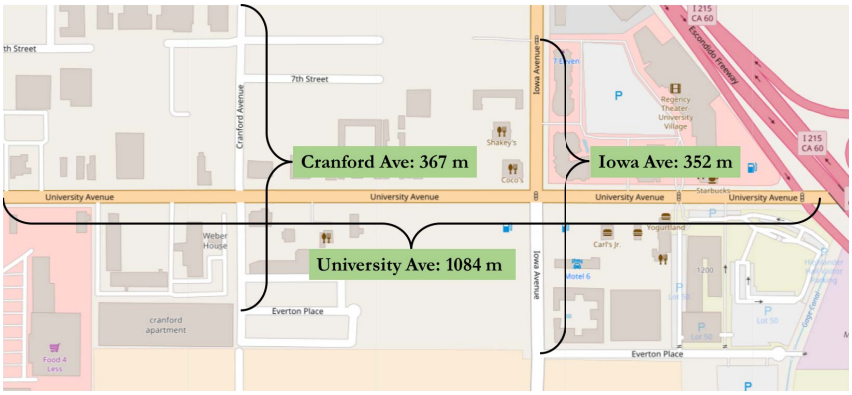

Fig. 3. Road segments in Riverside, CA that are modeled in this simulation study.

TABLE I

SIGNAL TIMING DATA OF CRANFORD AVENUE & UNIVERSITY AVENUE INTERSECTION

Intersection	Direction	Signal Phase (denoted by color) and Timing (in second)									
Cranford Avenue & University Avenue	North Through	0~23			23~60		60~64	64~100			
	South Through										
	East Left	0~5	5~18	18~22	22~100						
	East Through	0~4	4~80								80~100
	West Left	0~65							65~75	75~79	79~100
	West Through	0~4	4~65						65~100		

TABLE II

SIGNAL TIMING DATA OF IOWA AVENUE & UNIVERSITY AVENUE INTERSECTION

Intersection	Direction	Signal Phase (denoted by color) and Timing (in second)									
Iowa Avenue & University Avenue	North Through	0~39				39~68		68~72	72~100		
	South Through										
	North Left	0~21			21~34	34~38	38~100				
	South Left										
	East Left	0~5	5~16	16~20	20~100						
	East Through	0~16		16~20	20~87						87~100
	West Left	0~73							73~82	82~86	86~100
	West Through	0~4	4~73						73~100		

Algorithm 3: Estimated Time-to-Arrival of the CED Follower

Input: available green window T, CED leader's estimated time-to-arrival t_{arr_l}, preceding vehicle's estimated time-to-arrival t_{arr_p}, position of the ego CED follower in the string n, length of a red phase t_{red}, length of an amber phase t_{amber}, desired time headway $t_{headway}$

Output: estimated time-to-arrival t_{arr}

```
for all CED followers in the V2I range do
    t_arr_temp = t_arr_l + n · t_headway
    if t_arr_temp ∈ T then
        t_arr = t_arr_temp
    else
        if t_arr_p ∈ T then
            t_arr = t_arr_p + t_amber + t_red
        else
            t_arr = t_arr_p + t_headway
        end if
    end if
end for
```

V. SIMULATION AND DISCUSSION

We conduct a simulation study on the proposed CED system and evaluate its system-wide impacts. The simulation network is built based upon the six-mile University Avenue corridor in Riverside, California. We focus on the intersections of University & Cranford, and University & Iowa, where the specific road segments modeled in this simulation study can be illustrated in Fig. 3. The particular segments of roads that lie between two ends of each black brace are built in traffic simulation environment, where University Avenue has a length of 1084 m, Cranford Avenue has a length of 367 m, and Iowa Avenue has a length of 352 m. The data of signal timing and traffic count on these two intersections are provided by the City of Riverside. Specifically, we use the data collected during 7:00-8:00 AM on Thursday, June. 2nd, 2016 to calibrate the inputs of our simulation network. We select this period since we want to simulate a morning-peak traffic network in a typical weekday. The signal timing data are shown in TABLE I and TABLE II, and the traffic count data are shown in TABLE III.

We adopt PTV VISSIM, a microscopic multi-modal traffic flow simulation software, to build the simulation network of the proposed CED system [26]. Specifically, VISSIM Application Programmer's Interface (API) package enables users to integrate external applications to take influence on the traffic simulation. In this research, we implement the proposed role transition and longitudinal models in the

Authorized licensed use limited to: Univ of Calif Riverside. Downloaded on April 14,2020 at 21:38:26 UTC from IEEE Xplore. Restrictions apply.

This article has been accepted for inclusion in a future issue of this journal. Content is final as presented, with the exception of pagination.

TABLE III
TRAFFIC COUNT DATA OF UNIVERSITY & CRANFORD INTERSECTION AND UNIVERSITY & IOWA INTERSECTION

Intersection	**University & Cranford Intersection**											
Direction	Northbound			Southbound			Eastbound			Westbound		
	Left	Through	Right	Left	Through	Right	Left	Through	Right	Left	Through	Right
Number of Lanes	0	1	0	0	1	0	1	2	1	1	2	0
Total Volumes	8	4	22	32	5	46	41	367	9	4	282	29
Intersection	**University & Iowa Intersection**											
Direction	Northbound			Southbound			Eastbound			Westbound		
	Left	Through	Right	Left	Through	Right	Left	Through	Right	Left	Through	Right
Number of Lanes	1	2	1	1	2	0	2	2	1	1	2	1
Total Volumes	56	502	54	113	214	102	138	246	31	49	163	91

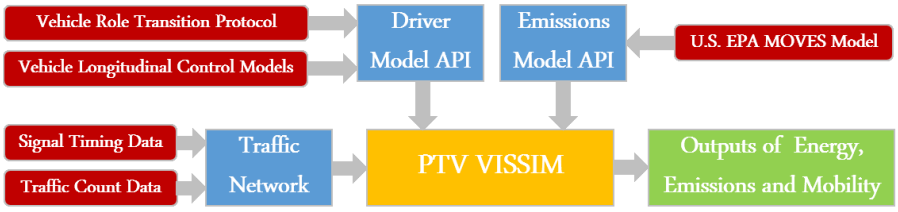

Fig. 4. System architecture of the simulation study in VISSIM.

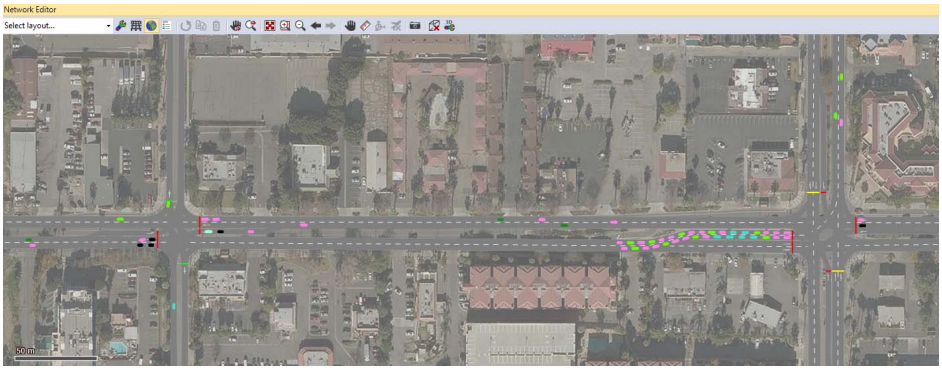

Fig. 5. University Avenue network built in VISSIM.

DriverModel.DLL, which can be assigned to specific vehicle types in VISSIM and overwrite the standard driving behavior. Additionally, the EmissionsModel.DLL is provided by VISSIM to add user-defined emission models, where we implement the U.S. Environmental Protection Agency's MOtor Vehicle Emission Simulator (MOVES)-based model to perform analysis on the environmental impacts of the system [32]. The overall architecture of this simulation study can be illustrated as Fig. 4.

The simulation traffic network built in VISSIM can be partially illustrated as Fig. 6 (2D mode) and Fig. 6 (3D mode). We use light green color for conventional vehicles, and several different colors for CED vehicles based on their scenarios (mainly for debugging and demonstration purposes). All signal controllers in the network are designed based on TABLE I and TABLE II, and vehicle volumes are set by TABLE III. Parameters of the traffic network and vehicles in this simulation study are listed in TABLE IV.

The microscopic traffic simulation results are shown in TABLE V, with two baseline scenarios (1) and (2) and ten CED scenarios (3)-(12). Specifically, we also include EAD-Only vehicles in scenario (2), which conduct EAD maneuvers in an ego manner. For EAD-only vehicles, only V2I communications are enabled where they can plan their speed trajectories based on the information received from the infrastructure. V2V communications are not enabled for them, which means they cannot cooperate with each other like CED vehicles. Note baseline scenario (2) already outperforms (1) in terms of all environmental measurements, as shown in TABLE V.

With respect to CED scenarios, positive impacts on NO_X, HC and CO can be observed at any penetration rate of CED vehicles in the traffic system. However, when there are less than 70% CED vehicles in the traffic system, negative impacts on energy and CO_2 can be observed compared to these two baseline scenarios. Especially, as can be seen from TABLE V, the worst scenario in terms of energy consumption and CO_2 emission is with 40% CED vehicles in the traffic network. There are basically two reasons for this behavior:

1) The introduction of CED vehicles brings about conservative driving behaviors to the traffic network: When they know they can travel through the intersection during the green window with current speed, they approach

Authorized licensed use limited to: Univ of Calif Riverside. Downloaded on April 14,2020 at 21:38:26 UTC from IEEE Xplore. Restrictions apply.

This article has been accepted for inclusion in a future issue of this journal. Content is final as presented, with the exception of pagination.

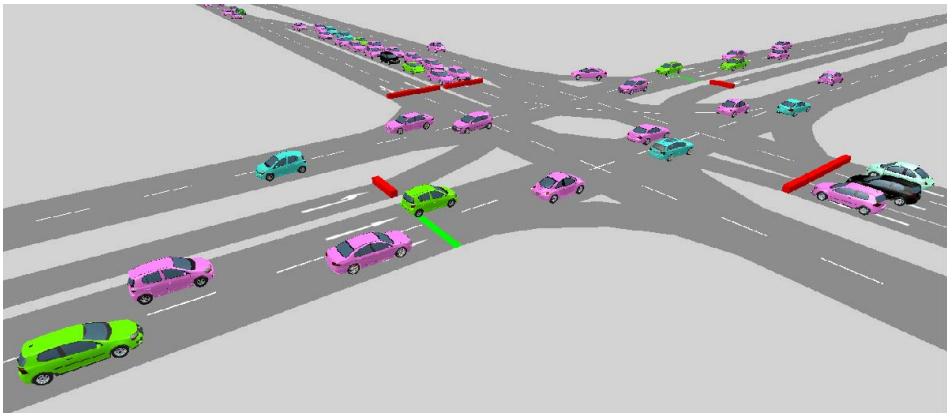

Fig. 6. Simulation is running in VISSIM with 3D mode.

TABLE IV
PARAMETERS OF THE SIMULATION TRAFFIC NETWORK AND VEHICLES

Parameters	Value	Parameters	Value
Simulation Date	June 2nd, 2016	Desired Speed of Vehicles v_{des}	20 m/s
Simulation Period	7:00 – 8:00 AM	Free Acceleration Exponent δ	4
Simulation Resolution	10 time steps/second	Damping Gain β	0.58
V2V Communication Range	100 m	Damping Gain γ	1
V2I Communication Range	300 m	Desired Time Gap t_{gap}	0.5 s
Average Standstill Distance $a \cdot x$	2 m	Minimum Allowed Inter-Vehicle Distance d_{safe}	3 m
Additive Part of Safety Distance $b \cdot x_{add}$	2 m	Maximum Allowed Jerk $jerk_{max}$	10 m/s^3
Multiplicative Part of Safety Distance $b \cdot x_{mult}$	3 m	Maximum Allowed Acceleration a_{max}	1.5 m/s^2
Coefficient z	0.5	Maximum Allowed Deceleration d_{max}	-2.5 m/s^2

TABLE V
SIMULATION RESULTS OF ENERGY CONSUMPTION AND POLLUTANT EMISSIONS

Scenario	Vehicle Composition	Energy		NO_X		HC		CO		CO_2	
(1)	0% CED &100% Conventional	3924.2 kJ/km		0.051 g/km		0.015 g/km		1.394 g/km		284.9 g/km	
(2)	0% CED & 100% EAD-Only	3737.5 kJ/km		0.044 g/km		0.013 g/km		1.254 g/km		271.3 g/km	
	Reductions ratio with respect to	Sce.(1)	Sce.(2)	Sce.(1)	Sce.(2)	Sce.(1)	Sce.(2)	Sce.(1)	Sce.(2)	Sce.(1)	Sce.(2)
(3)	10% CED &90% Conventional	-0.3%	-5.4%	7.3%	0.0%	7.8%	-1.2%	7.9%	6.1%	-0.3%	-5.4%
(4)	20% CED &80% Conventional	-3.1%	-8.2%	14.6%	7.9%	15.4%	7.1%	16.0%	6.1%	-3.1%	-8.2%
(5)	30% CED &70% Conventional	-4.0%	-9.2%	20.7%	14.5%	21.8%	14.2%	22.5%	-2.3%	-4.0%	-9.2%
(6)	40% CED &60% Conventional	-12.0%	-17.6%	25.6%	19.7%	26.2%	19.0%	27.8%	6.7%	-12.0%	-17.6%
(7)	50% CED &50% Conventional	-6.5%	-11.8%	33.3%	28.1%	34.4%	28.0%	35.5%	13.9%	-6.5%	-11.8%
(8)	60% CED &40% Conventional	-3.1%	-8.2%	37.9%	33.0%	39.6%	33.8%	40.9%	19.8%	-3.1%	-8.2%
(9)	70% CED &30% Conventional	-0.9%	-5.9%	42.5%	38.0%	44.3%	38.9%	45.2%	28.3%	-0.9%	-5.9%
(10)	80% CED &20% Conventional	3.9%	-0.9%	46.9%	42.8%	49.2%	44.3%	49.8%	34.3%	3.9%	-0.9%
(11)	90% CED &10% Conventional	6.5%	1.8%	49.9%	46.0%	51.0%	46.2%	54.5%	39.1%	6.5%	1.8%
(12)	100% CED	7.1%	2.5%	54.6%	51.1%	56.7%	52.5%	59.0%	44.3%	7.1%	2.5%

the intersection by cruising instead of accelerating. When they depart the intersection after a full stop during the red window, they conduct an eco-departure maneuver with low acceleration process to save energy. Such conservative driving behaviors surely impede the movements of conventional vehicles, which always try to travel through the intersection as fast as possible. A very good example of this can be observed in Fig. 6, specifically at the right intersection (Iowa Avenue & University Avenue). As can been seen from TABLE III, the volume of eastbound left-turn vehicles at that intersection during that one hour is 138, however, there is only an 11-second green window during a 100-second signal cycle on that direction (derived from TABLE II). Therefore, the relatively slow departure rate of CED vehicles introduces a long queue along the upstream of eastbound University Avenue, so many through vehicles have to make unnecessary speed changes/full stops and consume more energy.

2) Since the proposed cooperative eco-driving methodology focus on collaborations among different CED vehicles, when the penetration rate of CED vehicles in the traffic

Authorized licensed use limited to: Univ of Calif Riverside. Downloaded on April 14,2020 at 21:38:26 UTC from IEEE Xplore. Restrictions apply.

This article has been accepted for inclusion in a future issue of this journal. Content is final as presented, with the exception of pagination.

network is lower than some certain threshold, it is difficult for CED vehicles to connect with each other and conduct collaborative maneuvers, and therefore brings about negative impacts on energy consumption. Based on the simulation results, 40% is the threshold when CED vehicles are not enough in the traffic network to conduct cooperative eco-driving maneuver, so the energy consumption comes out as the worst case scenario. When the penetration rate of CED vehicles is higher than 40%, it starts to compensate the negative impacts on conventional vehicles, so the energy consumption becomes better.

As can be seen from TABLE V, when there are enough CED vehicles in the traffic system, positive environmental impacts are shown. Specifically, compared to baseline scenario (1), 3.9% reduction on energy consumption can be observed when there are 80% CED vehicles. When all vehicles are CED vehicles, 7.1% and 2.5% reduction on energy consumption can be observed compared to baseline scenario (1) and (2), respectively. These results indicate that, only when the penetration rate of CED vehicles in the traffic system is high enough, the proposed CED system can work efficiently with more CED followers, instead of conventional vehicles, follow the movements of CED leaders and conduct eco-driving in a cooperative manner. It shall also be noted that CACC maneuver introduces energy savings for string followers since the reduction of their aerodynamic drag, but this factor is not included in the MOVES-based model. Therefore, if we consider aerodynamic drag of vehicle in the energy consumption model, the proposed system will get further reductions of energy consumption and pollutant emissions.

VI. Conclusions and Future Work

In this study, we have developed a CED system in a partially CAV environment, aiming to reduce energy consumption and pollutant emissions along a corridor with signalized intersections. Role transition protocol and longitudinal control models have been developed for different vehicles of the system. A microscopic traffic simulation has been conducted in PTV VISSIM with realistic traffic inputs, such as signal timing data and traffic count data. Simulations have been run with different penetration rates of CED vehicles, and their effects on traffic mobility have been evaluated. The MOVES model has been integrated to evaluate the environmental effects of the proposed CED system, where more than 7% reduction on energy consumption and up to 59% reduction on pollutant emission have been shown at 100% penetration rate of CED vehicles, respectively, when compared to the baseline.

Based on the simulation results and our analysis in Section V, there are several future work can be conducted to improve the proposed cooperative eco-driving system, especially to compensate the negative impacts when the penetration rate of CED vehicles is relatively low:

1) A joint vehicle-infrastructure eco-driving system can be developed based on the current version, where traffic signals can be designed to cooperate with CAVs under different traffic volumes and congestion levels to maximize the energy efficiency of the whole system. For example, the green window at University & Iowa intersection on eastbound left-turn direction can be rationally increased, given the relatively large traffic volumes on that direction.
2) The eco-departure algorithm of this cooperative eco-driving system can be further improved with the consideration of upstream queue length. If upstream vehicles are already waiting in a long queue, the CED vehicle may adopt a relatively quicker departure algorithm to allow more upstream vehicles to be discharged during the same green window.
3) Queue prediction algorithm can also be integrated to the eco-approach algorithm, so the estimated time-to-arrival value can be calculated more precisely, and the EAD scenario of the CED leader can be set more accurately. In such a manner, the dynamically changing queue length at the downstream intersection will less likely to introduce frequent speed changes of the approaching CED leader, and hence further reduce energy consumption.

Acknowledgements

The authors sincerely thank the City of Riverside for providing the traffic and signal data on University Avenue, Riverside.

References

[1] INRIX. *Los Angeles Tops INRIX Global Congestion Ranking*. Accessed: Feb. 9, 2018. [Online]. Available: http://inrix.com/press-releases/scorecard-2017/

[2] National Safety Council. *NSC Motor Vehicle Fatality Estimates*. Accessed: Feb. 9, 2018. [Online]. Available: http://www.nsc.org/NewsDocuments/2017/12-month-estimates.pdf

[3] U.S. Department of Transportation. *Bureau of Transportation Statistics*. Accessed: Jun. 17, 2017. [Online]. Available: https://www.rita.dot.gov/bts/sites/rita.dot.gov.bts/files/publications/transportation_statistics_annual_report/2015/chapter7.html

[4] Center for Advanced Automotive Technology. *Connected and Automated Vehicles*. Accessed: Feb. 12, 2018. [Online]. Available: http://autocaat.org/Technologies/Automated_and_Connected_Vehicles/

[5] K. Katsaros, R. Kernchen, M. Dianati, and D. Rieck, "Performance study of a green light optimized speed advisory (GLOSA) application using an integrated cooperative ITS simulation platform," in *Proc. IEEE 7th IWCMC*, Jul. 2011, pp. 918–923.

[6] G. De Nunzio, C. C. de Wit, P. Moulin, and D. Di Domenico, "Eco-driving in urban traffic networks using traffic signal information," in *Proc. IEEE Conf. Decision Control*, Florence, Italy, Dec. 2013, pp. 892–898.

[7] Y. Saboohi and H. Farzaneh, "Model for developing an eco-driving strategy of a passenger vehicle based on the least fuel consumption," *Appl. Energy*, vol. 86, no. 10, pp. 1925–1932, 2009.

[8] H. Xia, K. Boriboonsomsin, and M. Barth, "Dynamic ECO-driving for signalized arterial corridors and its indirect network-wide energy/emissions benefits," *J. Intell. Transp. Syst.*, vol. 17, no. 1, pp. 31–41, 2013.

[9] O. Altan, G. Wu, M. J. Barth, K. Boriboonsomsin, and J. Stark, "GlidePath: Eco-friendly automated approach and departure at signalized intersections," *IEEE Trans. Intell. Vehicles*, vol. 2, no. 4, pp. 266–277, Nov. 2017.

[10] X. Xiang, K. Zhou, W. B. Zhang, W. Qin, and Q. Mao, "A closed-loop speed advisory model with driver's behavior adaptability for eco-driving," *IEEE Trans. Intell. Transp. Syst.*, vol. 16, no. 6, pp. 3313–3324, Dec. 2015.

Authorized licensed use limited to: Univ of Calif Riverside. Downloaded on April 14,2020 at 21:38:26 UTC from IEEE Xplore. Restrictions apply.

This article has been accepted for inclusion in a future issue of this journal. Content is final as presented, with the exception of pagination.

[11] J. Lee and B. Park, "Development and evaluation of a cooperative vehicle intersection control algorithm under the connected vehicles environment," *IEEE Trans. Intell. Transp. Syst.*, vol. 13, no. 3, pp. 81–90, Mar. 2012.
[12] S. I. Guler, M. Menendez, and L. Meier, "Using connected vehicle technology to improve the efficiency of intersections," *Transp. Res. C, Emerg. Technol.*, vol. 46, pp. 121–131, Sep. 2014.
[13] Y. Feng, K. L. Head, S. Khoshmagham, and M. Zamanipour, "A real-time adaptive signal control in a connected vehicle environment," *Transp. Res. C, Emerg. Technol.*, vol. 55, pp. 460–473, Jun. 2015.
[14] B. van Arem, C. J. G. van Driel, and R. Visser, "The impact of cooperative adaptive cruise control on traffic-flow characteristics," *IEEE Trans. Intell. Transp. Syst.*, vol. 7, no. 4, pp. 429–436, Dec. 2006.
[15] V. Milanés, S. E. Shladover, J. Spring, C. Nowakowski, H. Kawazoe, and M. Nakamura, "Cooperative adaptive cruise control in real traffic situations," *IEEE Trans. Intell. Transp. Syst.*, vol. 15, no. 1, pp. 296–305, Feb. 2014.
[16] J. Ploeg, B. T. M. Scheepers, E. van Nunen, N. van de Wouw, and H. Nijmeijer, "Design and experimental evaluation of cooperative adaptive cruise control," in *Proc. 14th Int. IEEE Conf. Intell. Transp. Syst.*, Oct. 2011, pp. 260–265.
[17] Z. Wang, G. Wu, and M. J. Barth, "Developing a consensus-based cooperative adaptive cruise control (CACC) system for heterogeneous vehicles with predecessor following topology," *J. Adv. Transp.*, vol. 2017, Aug. 2017, Art. no. 1023654. doi: 10.1155/2017/1023654.
[18] Z. Wang, G. Wu, P. Hao, K. Boriboonsomsin, and M. Barth, "Developing a platoon-wide eco-cooperative adaptive cruise control (CACC) system," in *Proc. IEEE Intell. Vehicles Symp.*, Jun. 2017, pp. 1256–1261.
[19] Z. Wang, G. Wu, and M. J. Barth, "A review on cooperative adaptive cruise control (CACC) systems: Architectures, controls, and applications," in *Proc. IEEE 21st Int. Conf. Intell. Transp. Syst.*, Nov. 2018, pp. 2884–2891.
[20] S. Maiti, S. Winter, and L. Kulik, "A conceptualization of vehicle platoons and platoon operations," *Transp. Res. C, Emerg. Technol.*, vol. 80, pp. 1–19, Jul. 2017.
[21] Y. Meng, L. Li, F.-Y. Wang, K. Li, and Z. Li, "Analysis of cooperative driving strategies for nonsignalized intersections," *IEEE Trans. Veh. Technol.*, vol. 67, no. 4, pp. 2900–2911, Apr. 2018.
[22] H. Yang, H. Rakha, and M. V. Ala, "Eco-cooperative adaptive cruise control at signalized intersections considering queue effects," *IEEE Trans. Intell. Transp. Syst.*, vol. 18, no. 6, pp. 1575–1585, Jun. 2017.
[23] D.-F. Xie, X.-M. Zhao, and Z. He, "Heterogeneous traffic mixing regular and connected vehicles: Modeling and stabilization," *IEEE Trans. Intell. Transp. Syst.*, to be published.
[24] K. J. Malakorn and B. Park, "Assessment of mobility, energy, and environment impacts of intellidrive-based cooperative adaptive cruise control and intelligent traffic signal control," in *Proc. IEEE Int. Symp. Sustain. Syst. Technol.*, May 2010, pp. 1–6.
[25] Z. Wang, G. Wu, P. Hao, and M. J. Barth, "Cluster-wise cooperative eco-approach and departure application for connected and automated vehicles along signalized arterials," *IEEE Trans. Intell. Vehicles*, vol. 3, no. 4, pp. 404–413, Dec. 2018.
[26] PTV Group. *PTV Vissim*. Accessed: Mar. 1, 2018. [Online]. Available: http://vision-traffic.ptvgroup.com/en-us/products/ptv-vissim/
[27] H. Jiang, J. Hu, S. An, M. Wang, and B. Park, "Eco approaching at an isolated signalized intersection under partially connected and automated vehicles environment," *Transp. Res. C, Emerg. Techn.*, vol. 79, pp. 290–307, Jun. 2017.
[28] B. Asadi and A. Vahidi, "Predictive cruise control: Utilizing upcoming traffic signal information for improving fuel economy and reducing trip time," *IEEE Trans. Control Syst. Technol.*, vol. 19, no. 3, pp. 707–714, May 2011.
[29] M. A. S. Kamal, S. Taguchi, and T. Yoshimura, "Intersection vehicle cooperative eco-driving in the context of partially connected vehicle environment," in *Proc. IEEE 18th Int. Conf. Intell. Transp. Syst.*, Sep. 2015, pp. 1261–1266.
[30] R. Wiedemann, "Simulation des strassenverkehrsflusses," Inst. Transp. Sci., Univ. Karlsruhe, Karlsruhe, Germany, 1974. [Online]. Available: https://trid.trb.org/view/59623
[31] M. Treiber, A. Hennecke, and D. Helbing, "Congested traffic states in empirical observations and microscopic simulations," *Phys. Rev. E, Stat. Phys. Plasmas Fluids Relat. Interdiscip. Top.*, vol. 62, no. 2, pp. 1805–1824, 2000.
[32] *MOVES2014a User Guide*, U.S. Environ. Protection Agency, Washington, DC, USA, Nov. 2015.

Ziran Wang (S'16) received the B.E. degree in mechanical engineering and automation from the Beijing University of Posts and Telecommunications in 2015. He is currently pursuing the Ph.D. degree in mechanical engineering with the College of Engineering–Center for Environmental Research and Technology, University of California at Riverside, Riverside. He was a Research Intern with the Toyota Infotechnology Center, Mountain View, CA, USA, in 2018. He is also a Research Assistant with the College of Engineering–Center for Environmental Research and Technology, University of California at Riverside. His research focuses on connected and automated vehicle technology, including V2X, ADAS, motion planning and control. He holds memberships in various societies, including the IEEE, the Society of Automotive Engineers (SAE), the Transportation Research Board (TRB), the International Chinese Transportation Professional Association (ICTPA), and the Chinese Overseas Transportation Association (COTA). He received the National Center for Sustainable Transportation (NCST) Dissertation Award in 2018.

Guoyuan Wu (M'09–SM'15) received the Ph.D. degree in mechanical engineering from the University of California at Berkeley, Berkeley, in 2010. He is currently an Associate Research Engineer with the Transportation Systems Research (TSR) Group, Bourns College of Engineering–Center for Environmental Research and Technology (CE–CERT), and an Associate Adjunct Professor in electrical and computer engineering with the University of California at Riverside. His research focuses on the development and evaluation of sustainable and intelligent transportation system (SITS) technologies, including connected and automated transportation systems (CATS), optimization and control of vehicles, and traffic modeling and simulation. He is a Board Member of the Chinese Institute of Engineers–Southern California Chapter (CIE-SOCAL) and a member of the Chinese Overseas Transportation Association (COTA). He is an Associate Editor of the *SAE International Journal of Connected and Automated Vehicles* and also a member of the Vehicle-Highway Automation Committee (AHB30) of the Transportation Research Board (TRB).

Matthew J. Barth (M'90–SM'00–F'14) received the B.S. degree in electrical engineering/computer science from the University of Colorado in 1984 and the M.S. and Ph.D. degrees in electrical and computer engineering from the University of California at Santa Barbara, Santa Barbara, in 1985 and 1990, respectively.

He is currently the Yeager Families Professor with the College of Engineering, University of California at Riverside. He is a part of the intelligent systems faculty in electrical and computer engineering and is also serving as the Director of the Center for Environmental Research and Technology (CE-CERT). His research focuses on applying engineering system concepts and automation technology to transportation systems, and, in particular, how it relates to energy and air quality issues. His current research interests include ITS and the environment, transportation/emissions modeling, vehicle activity analysis, advanced navigation techniques, electric vehicle technology, and advanced sensing and control. He is active with the U.S. Transportation Research Board serving in a variety of roles in several committees, including the Committee on ITS and the Committee on Transportation Air Quality. He has also been active in the IEEE Intelligent Transportation System Society for many years, serving as a Senior Editor for both the *Transactions of ITS* and the *Transactions on Intelligent Vehicles*. He served as the IEEE ITSS President for 2014 and 2015 and is currently the IEEE ITSS Vice President for Finance.

Authorized licensed use limited to: Univ of Calif Riverside. Downloaded on April 14,2020 at 21:38:26 UTC from IEEE Xplore. Restrictions apply.